Features of programmed cell death in intact Xenopus oocytes and early embryos revealed by near-infrared fluorescence and real-time monitoring

CE Johnson[1], CD Freel[1] and S Kornbluth*,[1]

Factors influencing apoptosis of vertebrate eggs and early embryos have been studied in cell-free systems and in intact embryos by analyzing individual apoptotic regulators or caspase activation in static samples. A novel method for monitoring caspase activity in living Xenopus oocytes and early embryos is described here. The approach, using microinjection of a near-infrared caspase substrate that emits fluorescence only after its proteolytic cleavage by active effector caspases, has enabled the elucidation of otherwise cryptic aspects of apoptotic regulation. In particular, we show that brief caspase activity (10 min) is sufficient to cause apoptotic death in this system. We illustrate a cytochrome *c* dose threshold in the oocyte, which is lowered by Smac, a protein that binds thereby neutralizing the inhibitor of apoptosis proteins. We show that meiotic oocytes develop resistance to cytochrome *c,* and that the eventual death of oocytes arrested in meiosis is caspase-independent. Finally, data acquired through imaging caspase activity in the Xenopus embryo suggest that apoptosis in very early development is not cell-autonomous. These studies both validate this assay as a useful tool for apoptosis research and reveal subtleties in the cell death program during early development. Moreover, this method offers a potentially valuable screening modality for identifying novel apoptotic regulators.

Apoptosis is a form of programmed cell death executed by caspases. These cysteine proteases exist in the cytosol as zymogens until death stimuli trigger their activation.[1] Apoptotic signals can originate from extracellular ligands binding to cell-surface death receptors (extrinsic pathway) or from internal cues (e.g., DNA damage) inducing mitochondrial release of cytochrome *c* (intrinsic pathway).[2] In both cases, the resulting adapter protein complexes recruit initiator caspases, leading to their dimerization-induced activation.[3] Effector caspases are then processed by initiator caspases, greatly enhancing their enzymatic activity, freeing them to cleave an array of cellular substrates resulting in cell dismantling.[4]

Further study of the biochemical intricacies governing apoptotic signaling pathways is warranted, given that dysregulation of apoptosis contributes to the development of several important human pathologies, such as cancer and neurodegeneration.[5] Monitoring caspase activation is a critical component of studying apoptotic death, and numerous techniques that measure caspase activity have been developed.[6] Traditionally, these have relied upon biochemical analyses of lysates prepared from a large numbers of cells. More recently, fluorescence resonance energy transfer (FRET)-based caspase substrates have been developed that enable monitoring of caspase activity in mammalian cells.[7,8] These assays generally implement cellular expression of a

construct encoding two fluorescent proteins linked by a short peptide containing a caspase cleavage site (e.g., DEVD); caspase activation in a cell results in the separation of the two fluorescent proteins and a consequent change in fluorescence emission ratios. Although a powerful tool, the strategy relies on treatment of cell populations with apoptosis-inducing drugs and fluorescence imaging (microscopy or flow cytometry) over many hours. Moreover, use of such genetically encoded FRET indicators to monitor developmental programmed cell deaths would require production of transgenic animals and robust expression during embryogenesis.

The Xenopus system has traditionally been used as a powerful tool for studying both early embryonic development and cell cycle control.[9,10] Given the critical role of apoptosis in developmental processes and the emerging interplay between cell cycle and cell death regulators, this system has great potential to aid in the delineation of these crucial connections. Although extracts prepared from Xenopus eggs develop caspase activity over time (that can be monitored using a variety of fluorescent and colorimetric indicators *in vitro*), these activities reflect the 'death' of multiple pooled eggs in aggregate, rather than the real-time apoptosis of individual cells.[11] Microinjection of cytochrome *c* into Xenopus oocytes was shown to reliably induce apoptosis, but detection of death depended on changes in oocyte morphology (which take hours to occur) or on indirect markers of caspase

---

Department of Pharmacology and Cancer Biology, Duke University Medical Center, Durham, NC, USA
*Corresponding author: S Kornbluth, Department of Pharmacology and Cancer Biology, Duke University Medical Center, C370 LSRC, Research Drive, Durham, NC 27710, USA. Tel: 919 613 8624; 919 681 1005; E-mail: kornb001@mc.duke.edu

activation (e.g., plasma membrane depolarization).[12] Unfortunately, changes in membrane potential are not specific for apoptotic death, lack the sensitivity of the cell-free system, and cannot be recorded for more than one oocyte at a time. Thus, to date, there has been no means for directly measuring caspase activity in an intact Xenopus oocyte or early embryo.

Here, we report a novel method based on a near-infrared dye caspase substrate that allows measurement of caspase activation in real-time in living Xenopus oocytes. By applying this technique we have studied the kinetics of caspase activation, assessed the role of the inhibitor of apoptosis proteins (IAPs) in determining sensitivity to cytochrome *c*, compared caspase activation during different phases of the cell cycle, and imaged caspase activity in the early Xenopus embryo. These studies have revealed important subtleties in apoptotic regulation and also suggest the utility of this system as a tool for identifying novel apoptotic regulators.

Results

A near-infrared caspase substrate enables the detection of caspase activity in Xenopus oocytes.

Recently, a near-infrared (NIR) caspase substrate became commercially available from LI-COR, Inc.[13] This IRDye 800CW/QC-1 CSP-3 substrate (IRDye) emits fluorescence only after being cleaved by effector caspases at a canonical DEVD cleavage motif, which separates non-fluorescent quencher and NIR donor dyes, thereby restoring the donor signal (Figure 1a). To determine if the IRDye would be suitable for detecting caspase activity in intact Xenopus oocytes, we microinjected oocytes with cytochrome *c* and the IRDye. As controls, we microinjected either IRDye, cytochrome *c*, or IRDye and *Saccharomyces cerevisiae* cytochrome *c* (yeast cytochrome *c*), which is structurally similar to mammalian cytochrome *c*, but lacks the ability to trigger caspase activation.[14] The NIR fluorescence of microinjected (or untreated control) oocytes was imaged and results are shown in Figure 1b. Signal detected in the 700 nm channel was caused by oocyte autofluorescence (each red spot represents a single oocyte) whereas the 800 nm signal resulted from fluorescence of cleaved IRDye, with intense signal emanating from oocytes co-injected with cytochrome *c* and the IRDye (Figure 1c). These data strongly suggest that this method is well-suited for detecting caspase activity in intact oocytes. Designating the signal obtained from oocytes co-injected with yeast cytochrome *c* and IRDye as
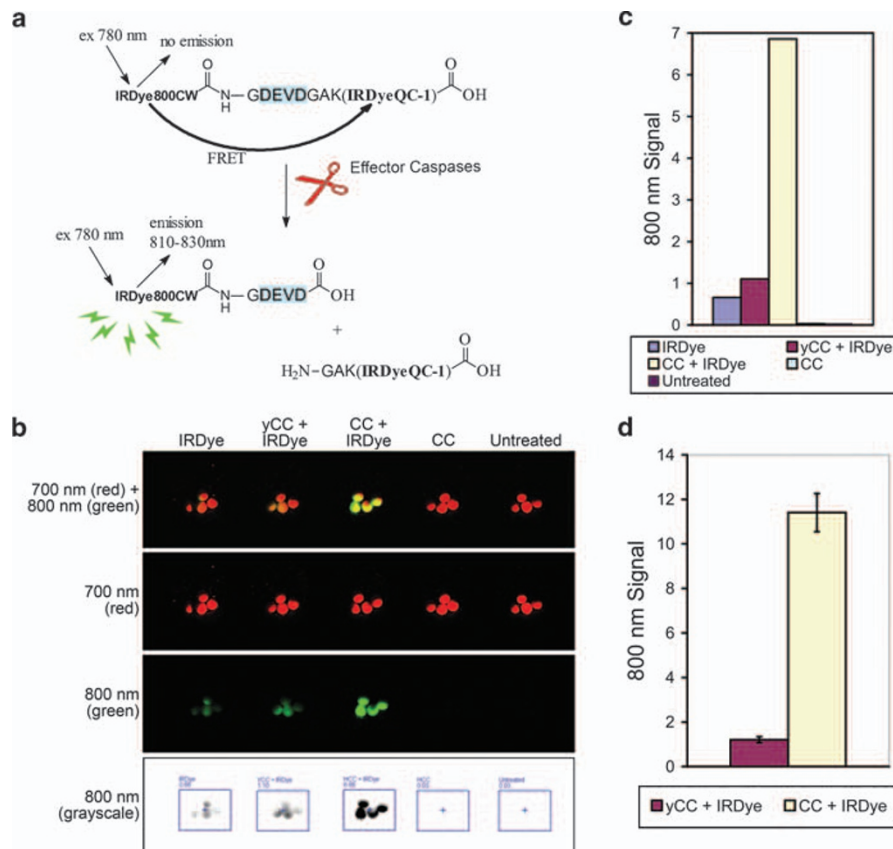

Figure 1 Fluorescence can be detected in oocytes microinjected with the IRDye and cytochrome *c*. (**a**) Schematic of the LI-COR IRDye 800CW/QC-1 CSP-3, which contains a non-fluorescent quencher dye (IRDyeQC-1) conjugated to a donor dye (IRDye800CW) by a DEVD-containing peptide. Proteolytic cleavage by active effector caspases separates the dyes, abolishing fluorescence resonance energy transfer (FRET) thereby restoring the donor dye fluorescence. Adapted with permission from LI-COR, Inc. (**b**) Oocytes were injected as indicated and imaged 30 min later. yCC, yeast cytochrome *c*, and CC, cytochrome *c*, both injected at 67 nM. (**c**) Graphical representation of the total quantitated signal in the 800 nm channel for each collective group of oocytes from B. Signal from individual oocytes in B can also be measured to calculate the average oocyte fluorescence (Supplementary Figure 1a and b). (**d**) Total quantitated signal in the 800 nm channel for each collective group of oocytes was averaged from independent microinjection experiments (*n* = 21) of IRDye with either yCC or CC and is displayed +/−S.E.M.

background, oocytes co-injected with cytochrome *c* and IRDye reliably yielded a ninefold signal increase above the background when imaged 30 min to 1 h after microinjection (Figure 1d). Additionally, this method allows the fluorescence of each individual oocyte to be measured (Supplementary Figure 1a), such that the average fluorescence intensity of the oocytes for each treatment can be calculated (Supplementary Figure 1b).

To show that the observed oocyte fluorescence truly reflected caspase activation, we first asked whether the signal could be negated by a caspase inhibitor or induced by factors that trigger the release of endogenous cytochrome *c*. Microinjection of the broad-spectrum caspase inhibitor z-VAD-fmk inhibited the signal whereas microinjection of tBid, a truncated form of Bid that induces cytochrome *c* release from mitochondria,[15] produced a signal comparable to that of the microinjected cytochrome *c* (Figure 2a). Furthermore, expression of Bok, a multi-domain pro-apoptotic member of the Bcl-2 family implicated in cell death in the ovary,[16] triggered apoptosis in oocytes that could be detected by the IRDye signal (Figure 2b). In addition, we prepared cell-free lysates from cytochrome *c*-microinjected oocytes to confirm the presence of active caspases, which we analyzed using both an *in vitro* colorimetric caspase assay (Figure 2c) and immunoblotting of active caspase-3 (Figure 2d). In aggregate, these data validate microinjection of the IRDye as a robust technique for imaging caspase activity within intact oocytes.

Caspases are rapidly activated and long-acting, but are required for a limited time to ensure cell death. The morphological changes that occur during apoptosis in Xenopus oocytes have been described previously.[12] In response to microinjected cytochrome *c,* oocytes initially appear unchanged, but approximately 2 h post-injection they develop mottling of the animal pole pigment (Figure 3a). Once an oocyte shows this characteristic morphological feature it will invariably die, but it is thought that caspase activation commits the cell to an apoptotic death before any detectable change in morphology.[4] Caspase activation in response to cytosolic cytochrome *c* is thought to be a rapid event,[17] and indeed, the IRDye-based *in vivo* oocyte caspase assay characterized above yielded detectable fluorescence within 5 min of cytochrome *c* microinjection (Figure 3b). This IRDye-based signal was detected for more than 24 h after microinjection, suggesting that the cleaved IRDye remained stable within the dying cell (Figure 3c). Microinjection of cytochrome *c* alone followed by microinjection of the IRDye at various time points resulted in a fluorescent signal for at least 4.5 h after exposure to cytochrome *c,* suggesting that caspases remain active and capable of cleaving substrates throughout the apoptotic process (Figure 3d).

To evaluate how long caspase activity must be maintained to cause apoptotic death (i.e., the 'point of no return') we microinjected cytochrome *c* followed by co-injection of IRDye and z-VAD-fmk at 10 min intervals. As shown in Figure 3e, z-VAD-fmk effectively inhibited caspase activity as detected by quenching of detectable IRDye fluorescence. Remarkably, cytochrome *c*-injected oocytes whose caspase activity was inhibited after 10, 20 or 30 min all showed apoptotic death,
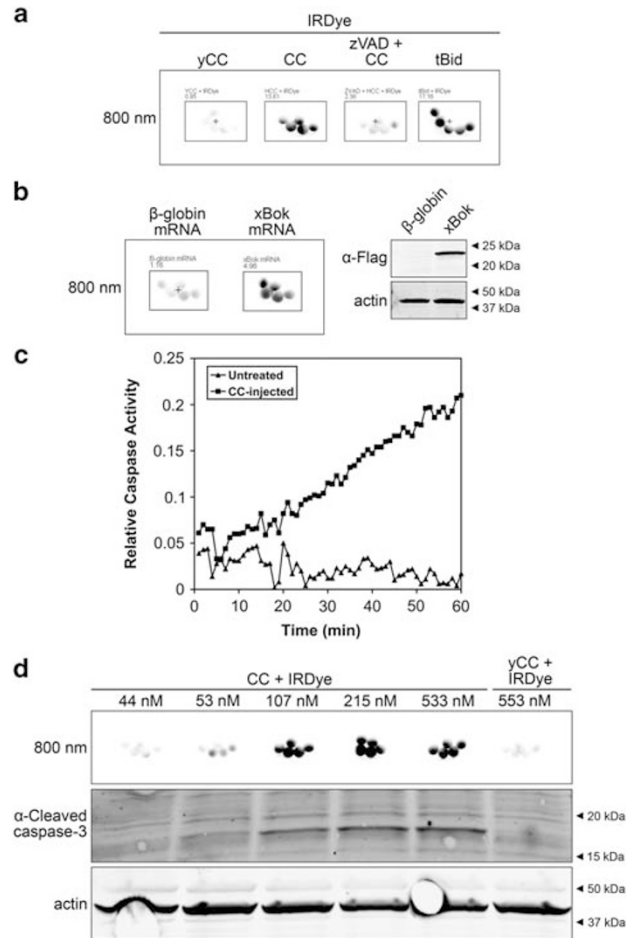

Figure 2 Oocyte fluorescence is due to activation of caspases. (**a**) Oocytes were injected with the IRDye and either yCC (267 nM), CC (267 nM), CC (267 nM) + z-VAD-fmk (40 nM), or tBid (167 nM) and imaged after 1 h. Average oocyte fluorescence is displayed in Supplementary Figure 1c. (**b**) Left, IRDye and 20 ng of either B-globin or flag-tagged Xenopus Bok (xBok) mRNA was injected into oocytes, allowed to express for 5 h at room temperature and then imaged. Average oocyte fluorescence is displayed in Supplementary Figure 1d. Right, oocyte lysates immunoblotted with anti-flag antibody showed xBok expression. (**c**) Cell-free lysates were prepared from untreated or CC-injected oocytes, and analyzed for caspase activity over time after the addition of the colorimetric caspase substrate Ac-DEVD-pNA. (**d**) Top, oocytes were injected with the IRDye and increasing doses of CC or yCC and imaged after 1 h. Bottom, lysates prepared from these oocytes immunoblotted for active caspase 3

with the time to development of apoptotic morphology unchanged in the 20 and 30 min groups and only slightly delayed in the 10 min group (Figure 3f). These data suggest that as little as 10 min of caspase activity is sufficient to promote cleavage of critical substrates and ensure death of the oocyte.

Inhibitor of apoptosis proteins serve as a brake to apoptosis in oocytes. During the course of these studies, we observed the presence of a threshold value for intracellular cytochrome *c* concentration, below which caspases did not become active and oocytes remained healthy; this cytochrome *c* threshold seems to fall between 50 and 100 nM (Figure 2d). These data suggested either that there must be a 'buffer' preventing caspase activity in these
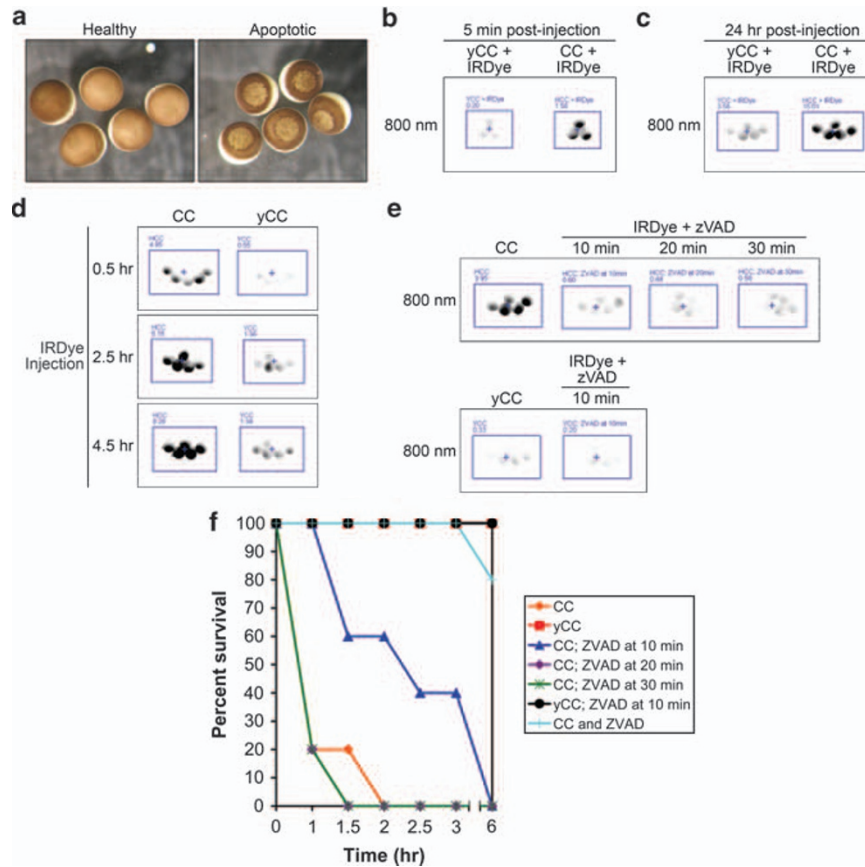
Figure 3 Caspases are rapidly activated in response to cytochrome *c*; caspases remain active for hours although their activity is only required for 10 min to ensure apoptosis. (**a**) Oocytes were injected with yCC (healthy) or CC (apoptotic) at 106 nM, and photographed 3 h later. (**b**) Oocytes microinjected with IRDye and either yCC or CC at 67 nM were imaged for fluorescence after 5 min, showing rapidity of the signal in response to even small amounts of CC. Average oocyte fluorescence is displayed in Supplementary Figure 1e. (**c**) Oocytes microinjected with IRDye and either yCC or CC at 533 nM were imaged after 24 h, showing a stable, selective induction of signal in CC-injected oocytes even at high yCC concentrations. Average oocyte fluorescence is displayed in Supplementary Figure 1f. (**d**) Oocytes microinjected with either CC or yCC at 80 nM at *t* = 0 were then injected with IRDye at various times indicated, and imaged 30 min later. Average oocyte fluorescence is displayed in Supplementary Figure 1g. (**e**) CC or yCC was microinjected at 533 nM at *t* = 0, then IRDye and z-VAD-fmk (70 nM) were injected at times indicated and then imaged 30 min later. Note z-VAD-fmk-mediated signal inhibition even at high concentrations of CC. Average oocyte fluorescence is displayed in Supplementary Figure 1h. (**f**) Survival curve based on observation of apoptotic morphology of oocytes that had been treated as described in E

cells and/or that the oocyte can tolerate a certain degree of caspase activity. In some systems (e.g., *Drosophila*), IAPs appear to have a critical role in determining cell survival/death. In vertebrates, it appears that IAPs have variable cell-type-specific roles, with a particular importance in setting the apoptotic threshold in differentiating cells such as maturing neuronal cells that harbor low levels of Apaf-1.[18] We hypothesized that IAP proteins might have a heretofore unsuspected role in setting the apoptotic threshold in the oocyte. To test this, we first confirmed expression of the two IAPs that have been described in Xenopus, XLX and xXIAP[19,20] (data not shown). We then microinjected oocytes with a sub-threshold dose of cytochrome *c* and Smac, a protein that functions as an inhibitor of IAP function.[21] Based on IRDye fluorescence, Smac addition substantially lowered the dose of cytochrome *c* required to induce caspase activation whereas heat-inactivated Smac had no effect (Figure 4a). In the presence of Smac, titration of the cytochrome *c* concentration to below 25 nM resulted in the failure of caspases to activate, suggesting the presence of a residual threshold that is IAP-independent (Figure 4b).

Careful analysis of the cytochrome *c* titration studies revealed that individual oocytes varied in their response to a peri-threshold dose. For example, in one particular batch of oocytes, 90 nM cytochrome *c*-induced caspase activation in 30% of oocytes, with IRDye fluorescence of three apoptotic and three living oocytes displayed in Figure 4c. Evaluation of IAP levels in these two sub-populations was performed with immunoblotting (Figure 4d). However, the striking differences in IAP quantities do not necessarily reflect differential expression levels because IAPs are rapidly degraded by active caspases that are present only in the apoptotic oocytes. Ideally we would compare sub-populations before cytochrome *c* microinjection, but unfortunately there is no means for predicting which oocytes will survive and which will die. As we have previously reported, an endogenous apoptotic program in oocytes, including mitochondrial cytochrome *c* release and caspase activation, is manifested when they are incubated on the bench, at least in part because they exhaust nutrient stockpiles required for viability.[22] We have observed that the presence of Smac hastens the induction of apoptosis in oocytes aged on the bench (data not shown), further
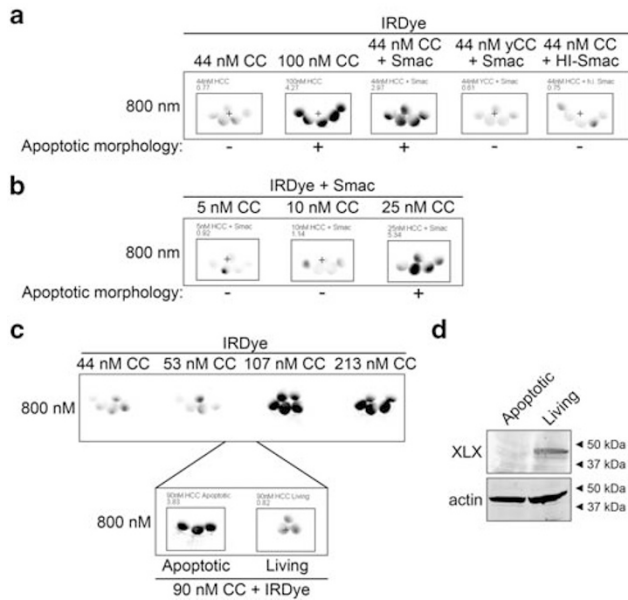
Figure 4 A cytochrome *c* threshold exists in oocytes and is lowered by Smac addition. (**a**) Oocytes were microinjected with IRDye and either sub-threshold CC (44 nM), supra-threshold level of CC (107 nM), 44 nM CC plus Smac protein, 44 nM yCC plus Smac, or 44 nM CC plus Smac that had been heat-inactivated by heating at 95 °C for 5 min (HI-Smac) and then imaged after 40 min. Smac was injected to a concentration of 280 nM. Average oocyte fluorescence is displayed in Supplementary Figure 1i. (**b**) Low doses of CC were injected with the IRDye and Smac and imaged after 30 min. Average oocyte fluorescence is displayed in Supplementary Figure 1j. (**c**) Oocytes were injected with IRDye and increasing doses of CC and imaged after 45 min. Naive oocytes from the same batch were then injected with IRDye and 90 nM CC, observed for apoptotic morphology and then three apoptotic and three living oocytes were imaged for fluorescence. Average oocyte fluorescence is displayed in Supplementary Figure 1k. (**d**) Lysates were prepared from the apoptotic and living oocyte groups described in C and then immunoblotted for XLX

supporting the hypothesis that IAP levels function as a brake to apoptosis in the oocyte.

Meiotic oocytes develop resistance to cytochrome *c*, and death of oocytes arrested in meiosis is caspase-independent. Stage VI Xenopus oocytes are arrested in G2 of the cell cycle. Treatment with progesterone (PG) induces oocyte maturation, which is marked by germinal vesicle breakdown (GVBD) and high cdc2 activity indicative of re-entry into the cell cycle.[23] GVBD results in a sharply demarcated loss of pigment in the animal pole, which, although distinct from apoptotic morphology, renders visual determination of whether a meiotic oocyte (post-GVBD) is undergoing apoptotic death challenging (Figure 5a). Using cell-free systems, we and others have reported that a meiotic state (M-phase) engenders resistance to cytochrome *c*-induced caspase activation.[24,25] A comparison of IRDye fluorescence in immature and mature (post-GVBD) oocytes microinjected with cytochrome *c* confirmed that sensitivity to cytochrome *c* decreases with maturation (Figure 5b). Approximately 30 min after stimulation with PG but well before GVBD, PG-treated and control oocytes displayed comparable sensitivity to cytochrome *c,* showing that PG is not simply disrupting the IRDye-based assay, and strengthening the notion that
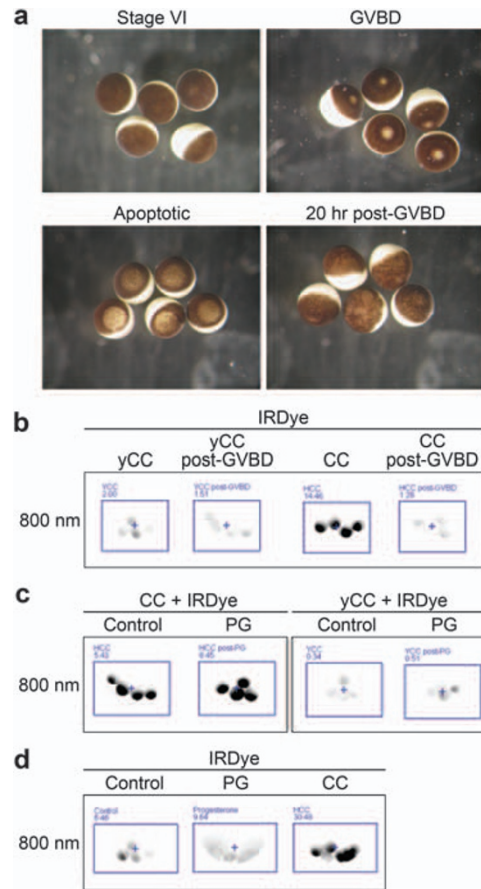

Figure 5 Progester-induced oocyte maturation decreases sensitivity to cytochrome *c*. (**a**) Reflected light images of healthy stage VI oocytes (top left), progesterone-treated oocytes showing GVBD (top right), cytochrome *c*-injected apoptotic oocytes (bottom left), and deteriorating unfertilized oocytes 20 h after GVBD (bottom left). (**b**) Oocytes were treated with progesterone and allowed to mature until GVBD, approximately for 5 h. Post-GVBD or control-treated oocytes were then injected with the IRDye and yCC or CC (at 67 nM), and then imaged after 1 h. Average oocyte fluorescence is displayed in Supplementary Figure 1. (**c**) Oocytes were treated with progesterone for 30 min before injecting them or control-treated oocytes with the IRDye and yCC or CC (at 533 nM), and imaged after 1 h. Average oocyte fluorescence is displayed in Supplementary Figure 1m. (**d**) Oocytes were treated with progesterone or control, microinjected with IRDye after GVBD and then imaged for fluorescence 24 h after progesterone treatment. Oocytes injected at the same time with IRDye and CC at 67 nM were included as a positive control. Average oocyte fluorescence is displayed in Supplementary Figure 1n

resistance develops with entry into M-phase (Figure 5c). Notably, mature oocytes, arrested in meiosis II, that are not fertilized within several hours slowly deteriorate and ultimately die (Figure 5a). To determine if such death is caspase-mediated (e.g., apoptotic), we evaluated IRDye-based fluorescence over time in PG-treated oocytes. We observed that even 24 h after PG treatment, when oocytes appeared, by morphological criteria, to be dying, there was no indication of caspase activity based on the absence of IRDye fluorescence (Figure 5d), suggesting that death in these oocytes proceeds by a process other than classical apoptosis.

Apoptosis is not cell-autonomous in the early Xenopus embryo. We sought to extend our studies beyond the oocyte to determine if we could image caspase activation in the early

embryo and to investigate if there were novel features of the apoptotic program at early times post-fertilization. Indeed, caspase activity was detected in fertilized eggs microinjected with IRDye and cytochrome *c* (Figure 6a). Furthermore, individual blastomeres within the embryo were visualized, as in Figure 6a, where it was evident that IRDye fluorescence was present in both blastomeres, as would be expected because microinjection occurred before cell division. In embryos with two blastomeres, we microinjected a single blastomere with IRDye and cytochrome *c*, and fluorescence was detected within half of the embryo, suggesting that the signal and therefore caspase activation was localized to the microinjected half of the embryo (Figure 6b). Surprisingly, under these circumstances morphological death occurred not only in the microinjected half of the embryo but also in the uninjected half, albeit with a slightly delayed time course (Figure 6c). To determine whether the observed death

of the uninjected blastomere involved caspase activity, we microinjected one blastomere with cytochrome *c* and the other with IRDye. Caspase-mediated fluorescence was detected in the IRDye-injected side, suggesting that cytochrome *c* introduction into one half of the embryo caused caspase activation on the opposite side (Figure 6d).

One explanation for this phenomenon would be movement of cytochrome *c* from one blastomere to the other via cytoplasmic bridges, which have been reported in the early Xenopus embryo.[26–28] To evaluate whether we could detect the presence of cytoplasmic bridges, we performed a series of experiments using microinjection of cell cycle-arresting proteins and fluorescent dyes. Initially we used Mos protein, which has been previously shown to arrest the development of one half of an embryo when microinjected,[29] and confirmed that in our hands we observe arrest of only one side of the embryo (Figure 6e).
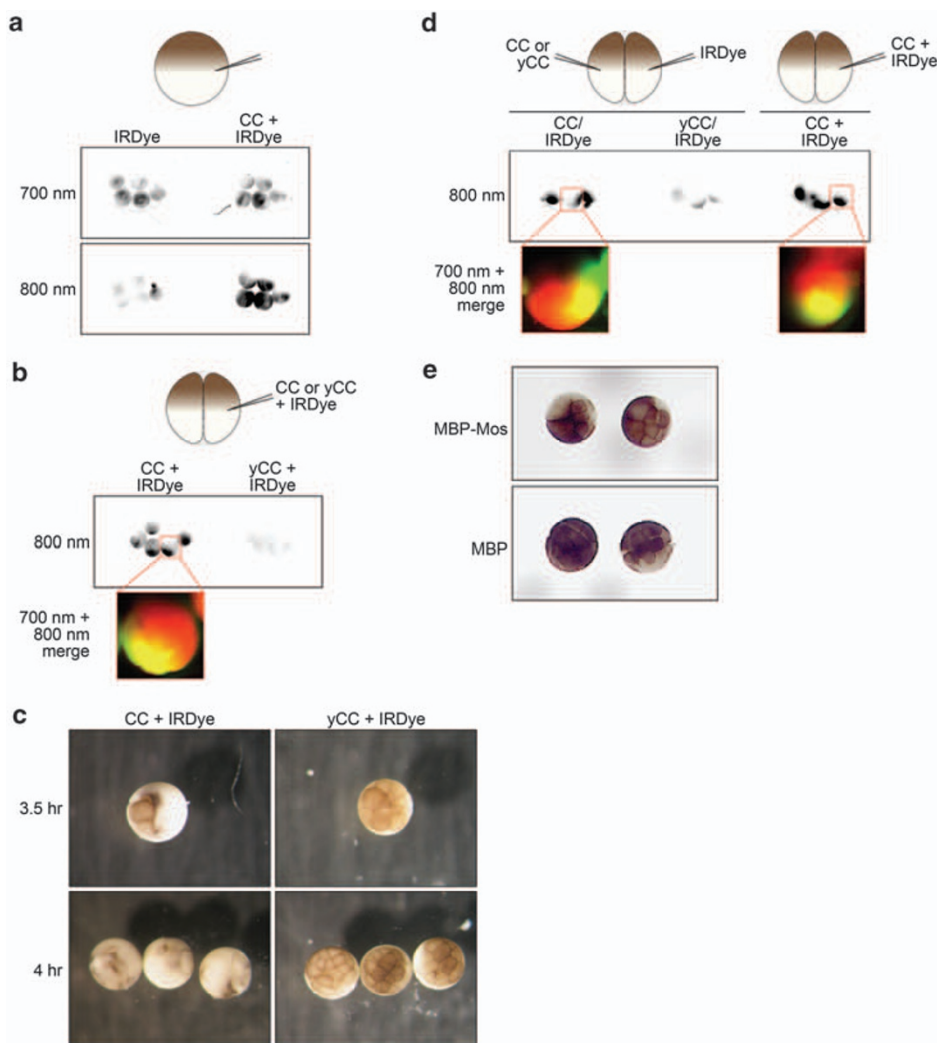

Figure 6 Cytochrome *c* injection of a single blastomere causes death of the entire embryo. (**a**) Fertilized eggs were injected before the first cell cleavage with the IRDye or IRDye and CC and then imaged during the two-cell stage. Autofluorescence is shown in the 700 nm channel and caspase activity in the 800 nm channel. (**b**) One blastomere of a two-cell embryo was microinjected with IRDye and either CC or yCC (at 270 nM), and imaged after 30 min (approximately 3 h after fertilization). (**c**) Embryos from B were photographed at the times indicated after fertilization. (**d**) Embryos were injected as indicated and then imaged 30 min later (approximately 3 h after fertilization). (**e**) Photographs of Mos-arrested or MBP control embryos, with left half arrested whereas right half of embryos continue to divide

Next, we took advantage of two fluorescent dextrans, one approximating the molecular weight of the IRDye (dextran, AF680 3000 MW) and one roughly the size of cytochrome *c* (dextran, AF680 10000 MW). Patterns of fluorescence in microinjected fertilized eggs *versus* single blastomeres of two-cell embryos were readily distinguishable, yielding a diffuse or partitioned signal, respectively (Figure 7a). We then micro-injected embryos at the two-cell stage, one blastomere receiving cytochrome *c* and the 3000 MW fluorescent dextran, and the opposite blastomere receiving the IRDye. As shown in Figure 7b, images of a single embryo illustrate 700 nm channel signal on one side (fluorescent dextran) and 800 nm
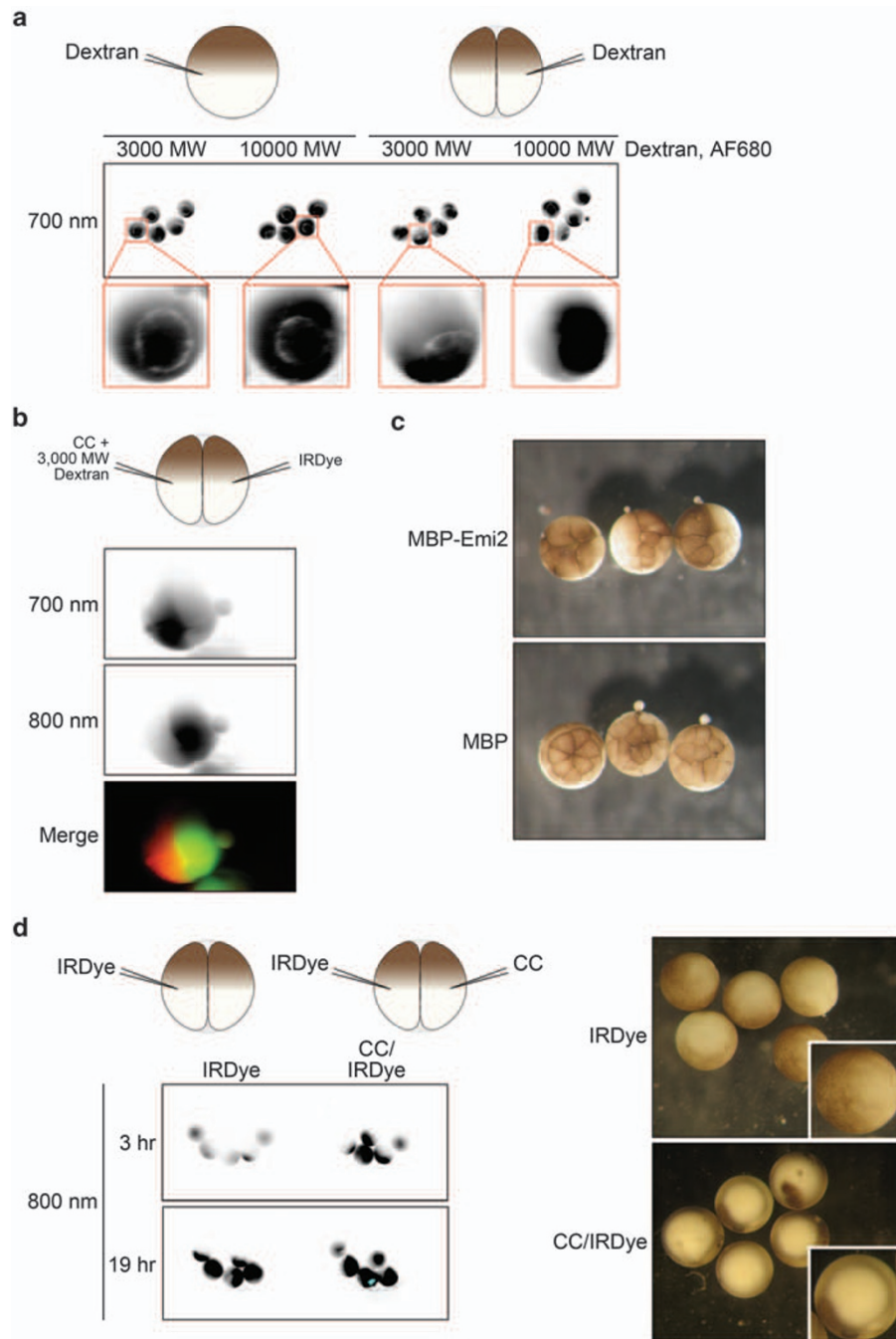

Figure 7 Apoptosis is not cell-autonomous in the early embryo. (**a**) Fluorescent dextrans were injected as indicated and then embryos were imaged 30 min later. (**b**) One embryo injected as indicated and imaged 30 min later. Signal in the 700 nm channel represents fluorescent dextran and signal in the 800 nm channel represents IRDye cleavage. (**c**) Emi2 mutant protein was injected into one blastomere at the two-cell stage and photographs were taken approximately 4 h post-fertilization. The embryo on the left shows full arrest, rather than arrest of only the injected side. (**d**) Left, embryos were injected as indicated (approximately 2 h post-fertilization) and imaged for fluorescence at the indicated times after fertilization. Right, photographs of the embryos 19 h post-fertilization, confirming IRDye-injected embryos are dividing normally and show no signs of apoptosis

channel signal on the other side (fluorescent IRDye), showing that transfer of dyes either does not occur or is not detectable with this methodology. Finally, we microinjected a concentrated preparation of an active, non-degradable fragment of Emi2 protein (aa 489–651 T545,551A), known to inhibit the anaphase-promoting complex, inducing a cell-cycle arrest similar to that of Mos protein.[30] In the large majority of microinjected embryos we observed the expected arrest of one half of the embryo, though in roughly one-third of cases we observed arrest of the entire embryo, which most likely reflects transfer of Emi2 across cytoplasmic bridges (Figure 7c). Presumably, transfer of injected Mos (Figure 6d) also occurred but the concentration was too low to induce an arrest on the uninjected side. Collectively, these data strongly suggest that apoptosis in the early embryo is not cell-autonomous as it is in later embryogenesis and adulthood, likely because of the presence of cytoplasmic linkages between blastomeres that is below detection by fluorescent dye imaging. These data are consistent with the notion that it is preferable to eliminate the entire embryo when apoptosis initiates in a single cell at a point in development when the dying cell represents a significant portion of the embryo.

Discussion

We employed microinjection of an NIR dye caspase substrate to measure caspase activity in individual, living Xenopus oocytes and early embryos in real-time. This assay provides quantitation of caspase activity that can be obtained rapidly (and repeatedly over time), and is easily distinguishable from oocyte maturation-induced GVBD. Relative to the traditional Xenopus cell-free system, this approach enables evaluation of individual cells, and has the unique strength of being able to monitor caspase activity and morphological apoptotic death in oocytes and developing embryos as separable entities (Figure 3e,f; Figures 6 and 7).

The Xenopus oocyte is easily microinjected and NIR imaging can be performed immediately following exposure to cytosolic cytochrome *c*. This enables us to address questions that have been technically impractical, a strength that is illustrated by our studies probing caspase activation kinetics. These experiments confirm that caspases become activated extremely rapidly in response to cytochrome *c* (in under 5 min). In addition, we investigated whether continued caspase activity is required to cause apoptosis. Our data indicate that even short-term activation of caspases (as brief as 10 min of exposure to cytosolic cytochrome *c*) causes an oocyte to die through apoptosis, suggesting that only caspase substrates cleaved within this timeframe are essential for cell dismantling. In light of the vast number of identified caspase substrates,[31,32] and the uncertainty of precisely how caspase-mediated proteolysis translates into organized cellular breakdown, this result yields insight into how caspase substrates might be prioritized for further functional characterization. Very recently, Edgington *et al.*[33] reported the development of activity-based fluorescent probes for imaging the kinetics of caspase activation *in vivo*. It would be of considerable interest to compare these reagents to the substrate used here for their resolution and sensitivity in our single-cell analyses.

In addition to the cytochrome *c*-induced caspase activity described, we also observed significant fluorescence of embryos microinjected with IRDye alone by 19 h after fertilization (Figure 7d). Sublethal caspase activity has been reported in Xenopus oocytes as well as in human preimplantation embryos,[34,35] and we hypothesize that our observations reflect the accumulation of minimal amounts of active caspases present at any given time that become significant only in summation. It is unclear whether these minimal amounts of caspase activity are important for development or are simply an inexorable consequence of rapid cell division that is tolerated by the embryo. Regardless, this observation prompted us to reflect upon our IAP studies, in which we saw that Smac addition, which we believe serves to neutralize IAPs in the oocyte, decreases the amount of cytochrome *c* required to activate caspases. Perhaps the levels of IAPs endowed to an oocyte determine whether an embryo will be able to limit the amount of caspase activation to within a tolerable range. One intriguing possibility warranting further investigation is that IAP levels decrease with age, making older oocytes more prone to apoptotic death following fertilization.

A series of studies performed in Xenopus embryos refer to the presence of cytoplasmic bridges between daughter cells.[26–28] Our studies in which we microinject cytochrome *c* into individual blastomeres and cause entire embryo apoptosis support this idea. It is well known that checkpoint activation does not occur in embryos until after the mid-blastula transition;[36] one important reason for such a delay might be to prevent the triggering of apoptosis by minor cellular damage during a time when death of an individual blastomere would lead to death of the entire embryo. Conversely, in the presence of a cell-damaging stimulus sufficiently strong to warrant induction of cell death in a single cell, it would likely be advantageous to rapidly induce death of the entire embryo to avoid significant developmental anomalies.

Although our experiments with microinjected cytochrome *c* and Emi2 strongly support the notion of communicating cytoplasms, we were unable to image this phenomenon using fluorescent dyes. So although this assay offers a powerful means for detecting caspase activity within a single cell, it may be that this imaging modality lacks the sensitivity required to detect a very weak signal when in direct proximity to a very strong one.

Although clearly advantageous for monitoring apoptosis as part of an inquiry into basic cellular and developmental processes, the technique presented here might also be employed as a screening modality to identify apoptotic regulators. The 96-well format combined with the ease of oocyte microinjection make this system poised for either medium-throughput or secondary screens. Given our previous reports suggesting that an apoptosome-stimulating therapeutic might be useful in the treatment of breast and brain tumors,[37,38] it may prove worthwhile to employ this assay to screen small-molecule libraries for a cytochrome *c* mimetic. Moreover, Xenopus oocytes have been used to good effect in screening small pool cDNA libraries for novel cell cycle regulators.[39] A similar approach, using the NIR dye as an apoptotic indicator, may allow identification of novel cell death-regulating proteins.

Materials and Methods

Molecular biology and chemicals. Standard molecular biology techniques were followed. Unless otherwise specified, chemicals and reagents were from Sigma-Aldrich (St Louis, MO, USA).

Cloning, protein expression and mRNA synthesis. Cloning, expression and purification of Mos and Emi2 (aa 489–651) T545,551A were as described.[40] Xenopus Bok (xBok) was cloned from an EST clone of the NIBB Xenopus laevis project. Initially xBok cDNA was amplified using an *Eco*RI forward primer (GGAATTCTAATGGAGATGCTAAGACGATC), and an *Xho*I reverse primer (GCTCGAGTTACCGCTCACGGAGGAC). For mRNA production, xBok was first cloned into the pSP64 T vector to contain an N-terminal FLAG tag. For mRNA synthesis, constructs were digested with *Sma*I or *Hind*III, and mRNAs produced using the mMessage mMachine RNA kit (Ambion, Austin, TX, USA).

Oocyte isolation, maturation and lysate preparation. Stage VI oocytes were prepared from ovaries manually excised from frogs primed with gonadotropin from pregnant mare serum (PMSG) (Calbiochem, San Diego, CA, USA), digested with 2.8 U of Liberase (Roche, Basel, Switzerland) in OR-2 buffer (82.5 mM NaCl, 2 mM KCl, 1 mM MgCl$_2$, 5 mM HEPES (pH 7.5)) for 1.5 h at room temperature, washed with OR-2 and stored in OR-2 + 10% fetal bovine serum (Invitrogen, Carlsbad, CA, USA) + 0.2% gentamicin (Invitrogen) at 18 °C. To induce maturation, oocytes were treated with 200 uM progesterone in OR-2. Oocyte lysate was made by crushing oocytes in oocyte lysis buffer (20 mM HEPES pH 7.5, 20 mM β-glycerophosphate, 15 mM MgCl$_2$, 20 mM EGTA, and 1 mM PMSF) followed by centrifugation to remove insoluble material. For western blot analysis, three oocyte equivalents were loaded per lane. For analysis of caspase activity, the lysate was diluted 10-fold with PBS, and incubated at 37 °C in the presence of the colorimetric substrate Ac-DEVD-pNA (Biomol, Plymouth Meeting, PA, USA). Absorbance was then measured using a Bio-Rad 680 microplate reader (Hercules, CA, USA) at 410 nm.

Xenopus *in vitro* fertilization. Testes were manually excised and used to fertilize fresh eggs laid from PMSG-primed frogs injected with human chorionic gonadotropin. Fertilized eggs were washed with 0.1 × MMR buffer (10 × MMR: 1 M NaCl, 20 mM KCl, 10 mM Mg SO$_4$, 25 mM Ca Cl$_2$, 5 mM HEPES pH 7.8, 0.8 mM EDTA), and then de-jellied following cortical rotation using 2% cysteine.

Microinjection. Oocytes were typically injected with 40 nl solution contained in a capillary needle using a PV830 pneumatic picopump (WPI, Berlin, Germany). If multiple rounds of injection were performed in a single cell, the injection volume was modified such that 40 nl was injected in total. Cytosolic volume of an oocyte was taken to be 1 ml, and used to calculate the final intracellular concentration of injected reagents. Microinjected reagents include: IRDye 800CW/QC-1 CSP-3 substrate (LI-COR, Lincoln, NE, USA) at 200–400 nM, cytochrome *c* from equine heart or from *Saccharomyces cerevisiae*, caspase-8-cleaved Bid (tBid) (Calbiochem) at 167 nM, z-VAD-fmk (Biomol) at 40–70 nM, human Smac protein (gift from Mohanish Deshmukh, University of North Carolina at Chapel Hill) used at 280 nM, dextran AlexaFluor680 3000 MW and dextran AlexaFluor 10 000 MW (Invitrogen). For mRNAs, 20 ng encoding β-globin or FLAG-xBok were injected per oocyte. For embryo injection, embryos were maintained in a solution of 0.3 × MMR buffer containing 4% Ficoll 400 (w/v); each blastomere was assumed to have a volume of 0.5 ml and was injected with 8 nl solution. All microinjection experiments included at least three oocytes/embryos per treatment group and each experiment was performed at least two independent times.

Immunoblotting. Antibodies used include: anti-flag (F3165, Sigma), anti-active caspase 3 (9661, Cell Signaling, Danvers, MA, USA), anti-actin (A1978, Sigma), anti-XLX serum (gift from Jean Gautier, Columbia University), and anti-xXIAP (gift from Shigeru Yamashita, Toho University). Alexa Fluor secondary antibodies (Invitrogen) were used with the Odyssey Infrared Imaging System (LI-COR).

Imaging. Infrared fluorescence in oocytes was imaged using the Odyssey Infrared Imaging system (LI-COR). Three to five oocytes per well in a black-walled 96-well plate (Corning Costar, Lowell, MA, USA) were scanned at a focus offset of 3.0 mm, resolution of 84 μm, and intensity settings of 5 in the 700 nm channel and 0.5 in the 800 nm channel. Embryos were imaged as above except at a resolution of 21 μm and intensity settings of either 5 or 2.5 in both channels. Analysis of fluorescence (including quantitation) was performed with the Odyssey software, v2.1 (LI-COR). Quantitation involved obtaining the total signal intensity for three to five oocytes per well. Reflected light images of oocytes and embryos were captured using a Stemi SV6 Stereomicroscope (Carl Zeiss, Thornwood, NY, USA) with an attached PowerShot A620 digital camera (Canon, Lake Success, NY, USA). Alternatively, a WolfVision Professional Visualizer (Duluth, GA, USA) was used to capture reflected light images of some of the embryos.

1. Earnshaw WC, Martins LM, Kaurmann SH. Mammalian caspases: structure, activation substrates, and functions during apoptosis. *Annu Rev Biochem* 1999; **68**: 383–424.
2. Schultz DR, Harrington Jr WJ. Apoptosis: programmed cell death at a molecular level. *Semin Arthritis Rhem* 2003; **32**: 345–369.
3. Shi Y. Activation of initiator caspases: history, hypotheses, and perspectives. *J Cancer Mol* 2005; **1**: 9–18.
4. Shi Y. Mechanisms of caspase activation and inhibition during apoptosis. *Mol Cell* 2002; **9**: 459–470.
5. Bellamy CO, Malcomson RD, Harrison DJ, Wyllie AH. Cell death in health and disease: the biology and regulation of apoptosis. *Semin Cancer Biol* 1995; **6**: 3–16.
6. Köhler C, Orrenius S, Zhivotovsky B. Evaluation of caspase activity in apoptotic cells. *J Immunol Methods* 2002; **265**: 97–110.
7. Rehm M, Dussmann H, Janicke RU, Tavare JM, Kogel D, Prehn JH. Single-cell fluorescence resonance energy transfer analysis demonstrates that caspase activation during apoptosis is a rapid process. Role of caspase-3. *J Biol Chem* 2002; **277**: 24506–24514.
8. Morgan MJ, Thorburn A. Measurement of caspase activity in individual cells reveals differences in the kinetics of caspase activation between cells. *Cell Death Differ* 2001; **8**: 38–43.
9. Jones CM, Smith JC. An overview of Xenopus development. *Methods Mol Biol* 2008; **461**: 385–394.
10. Philpott A, Yew PR. The Xenopus cell cycle. In: Humphrey TC and Brooks G (eds). *Cell cycle control: mechanisms and protocols*. Humana Press: New Jersey, 2005. pp 95–112.
11. Newmeyer DD, Farschon DM, Reed JC. Cell-free apoptosis in Xenopus egg extracts: inhibition of Bcl-2 and requirement for an organelle fraction enriched in mitochondria. *Cell* 1994; **79**: 353–364.
12. Bhuyan AK, Varshney A, Mathew MK. Resting membrane potential as a marker of apoptosis: studies on Xenopus oocytes microinjected with cytochrome c. *Cell Death Differ* 2001; **8**: 63–69.
13. Peng X, Chen H, Draney DR, Volcheck W, Schutz-Geschwender A, Olive DM. A non-fluorescent, broad range quencher dye for Förster resonance energy transfer assays. *Anal Biochem* 2009; **388**: 220–228.
14. Yu T, Wang X, Purring-Koch C, Wei Y, McLendon GL. A mutational epitope for cytochrome c binding to the apoptosis protease activation factor-1. *J Biol Chem* 2001; **276**: 13034–13038.
15. Li H, Zhu H, Xu CJ, Yuan J. Cleavage of BID by caspase 8 mediates the mitochondrial damage in the Fas pathway of apoptosis. *Cell* 1998; **94**: 491–501.
16. Hsu SY, Kaipia A, McGee E, Lomeli M, Hsueh AJ. Bok is a pro-apoptotic Bcl-2 protein with restricted expression in reproductive tissue and heterodimerizes with selective anti-apoptotic Bcl-2 family members. *Proc Natl Acad Sci USA* 1997; **94**: 12401–12406.
17. Berger AB, Witte MD, Denault JB, Sadaghiani AM, Sexton KM, Salvesen GS *et al.* Identification of early intermediates of caspase activation using selective inhibitors and activity-based probes. *Mol Cell* 2006; **23**: 509–521.
18. Wright KM, Linhoff MW, Potts PR, Deshmukh M. Decreased apoptosome activity with neuronal differentiation sets the threshold for strict IAP regulation of apoptosis. *J Cell Biol* 2004; **167**: 303–313.
19. Holley CL, Olson MR, Colón-Ramos DA, Kornbluth S. Reaper eliminates IAP proteins through stimulated IAP degradation and generalized translational inhibition. *Nat Cell Biol* 2002; **6**: 439–444.
20. Tsuchiya Y, Murai S, Yamashita S. Apoptosis-inhibiting activities of BIR family proteins in Xenopus egg extracts. *FEBS J* 2005; **272**: 2237–2250.
21. Deshmukh M, Du C, Wang X, Johnson Jr EM. Exogenous smac induces competence and permits caspase activation in sympathetic neurons. *J Neurosci* 2002; **22**: 8018–8027.

22. Nutt LK, Margolis SS, Jensen M, Herman CE, Dunphy WG, Rathmell JC *et al.* Metabolic regulation of oocyte cell death through the CaMKII-mediated phosphorylation of caspase-2. *Cell* 2005; **123**: 89–103.

23. Nebreda AR, Ferby I. Regulation of the meiotic cell cycle in oocytes. *Curr Opin Cell Biol* 2000; **12**: 666–675.

24. Allan LA, Clarke PR. Phosphorylation of caspase-9 by CDK1/cyclin B1 protects mitotic cells against apoptosis. *Mol Cell* 2007; **26**: 301–310.

25. Greenwood J, Gautier J. XLX is an IAP family member regulated by phosphorylation during meiosis. *Cell Death Differ* 2007; **14**: 559–567.

26. Byers TJ, Armstrong PB. Membrane protein redistribution during Xenopus first cleavage. *J Cell Biol* 1986; **102**: 2176–2184.

27. Cardellini P, Rasotto MB, Tertoolen LG, Durston AJ. Intercellular communication in the eight-cell stage of Xenopus laevis development: a study using dye coupling. *Dev Biol* 1988; **129**: 265–269.

28. Landesman Y, Goodenough DA, Paul DL. Gap junctional communication in the early Xenopus embryo. *J Cell Biol* 2000; **150**: 929–936.

29. Sagata N, Watanabe N, Vande Woude GF, Ikawa Y. The c-mos proto-oncogene product is a cytostatic factor responsible for meiotic arrest in vertebrate eggs. *Nature* 1989; **342**: 512–518.

30. Tung JJ, Hansen DV, Ban KH, Loktev AV, Summers MK, Adler 3rd JR *et al.* A role for the anaphase-promoting complex inhibitor Emi2/XErp1, a homolog of early mitotic inhibitor 1, in cytostatic factor arrest of Xenopus eggs. *Proc Natl Acad Sci USA* 2005; **102**: 4318–4323.

31. Dix MM, Simon GM, Cravatt BF. Global mapping of the tophography and magnitude of proteolytic events in apoptosis. *Cell* 2008; **134**: 679–691.

32. Mahrus S, Trinidad JC, Barkan DT, Sali A, Burlingame AL, Wells JA. Global sequencing of proteolytic cleavage sites in apoptosis by specific labeling of protein N termini. *Cell* 2008; **134**: 866–876.

33. Edgington LE, Berger AB, Blum G, Albrow VE, Paulick MG, Lieberry N *et al.* Noninvasive optical imaging of apoptosis by caspase-targeted activity-based probes. *Nat Med* 2009; **15**: 967–973.

34. Arnault E, Tosca L, Courtot AM, Doussau M, Pesty A, Finaz C *et al.* Caspase-2(L), caspase-9, and caspase-3 during *in vitro* maturation and fragmentation of the mouse oocyte. *Dev Dyn* 2008; **237**: 3892–3903.

35. Martinez F, Rienzi L, Iacobelli M, Ubaldi F, Mendoza C, Greco E *et al.* Caspase activity in preimplantation human embryos is not associated with apoptosis. *Human Reprod* 2002; **17**: 1584–1590.

36. Wroble BN, Sible JC. Chk2/Cds1 protein kinase blocks apoptosis during early development of Xenopus laevis. *Dev Dyn* 2005; **233**: 1359–1365.

37. Schafer ZT, Parrish AB, Wright KM, Margolis SS, Marks JR, Deshmukh M *et al.* Enhanced sensitivity to cytochrome c-induced apoptosis mediated by PHAPI in breast cancer cells. *Cancer Res* 2006; **66**: 2210–2218.

38. Johnson CE, Huang YY, Parrish AB, Smith MI, Vaughn AE, Zhang Q *et al.* Differential Apaf-1 levels allow cytochrome c to induce apoptosis in brain tumors but not in normal neural tissues. *Proc Natl Acad Sci USA* 2007; **104**: 20820–20825.

39. Ferby I, Blazquez M, Palmer A, Eritja R, Nebreda AR. A novel p34(cdc2)-binding and activating protein that is necessary and sufficient to trigger G(2)/M progression in Xenopus oocytes. *Genes Dev* 1999; **13**: 2177–2189.

40. Wu Q, Guo Y, Yamada A, Perry JA, Wang MZ, Araki M *et al.* A role for Cdc2- and PP2A-mediated regulation of Emi2 in the maintenance of CSF arrest. *Curr Biol* 2007; **17**: 213–224.

Supplementary Information accompanies the paper on Cell Death and Differentiation website (http://www.nature.com/cdd)